

ACOUSTO-OPTICS

PACS numbers: 42.79.Jq; 42.25.Fx; 42.70.Ce; 42.55.Lt
DOI: 10.1070/QE2015v045n10ABEH015667

Acousto-optic diffraction of multicolour Ar-laser radiation in crystalline quartz

V.M. Kotov, S.V. Averin, A.I. Voronko, P.I. Kuznetsov,
S.A. Tikhomirov, G.N. Shkerdin, A.N. Bulyuk

Abstract. **We have studied acousto-optic Bragg diffraction of multicolour radiation, generated by an Ar laser in the blue-green region of the spectrum, on an acoustic wave propagating in crystalline quartz. It is shown that crystalline quartz significantly exceeds commonly used paratellurite in terms of phase matching of optical beams with a single acoustic wave. We have performed experiments on pulse modulation of Ar-laser radiation. It is shown that distortions introduced into optical pulses are substantially less when use is made of a quartz crystal rather than paratellurite.**

Keywords: *acousto-optic diffraction, Bragg regime, multi-colour laser light.*

1. Introduction

Acousto-optic (AO) diffraction is widely used to control optical radiation – its amplitude, phase, frequency and polarisation [1–3]. The Bragg regime, which allows incident radiation to be deflected to one diffraction order with a high (close to 100%) efficiency, is most often used in practice. However, the high selectivity of the Bragg interaction with respect to the wavelength of light made it difficult until recently to use this regime to control multicolour laser light. Relatively recently, methods have been proposed to ensure Bragg diffraction of two-colour radiation on a single acoustic wave (see, e.g., [4–6]). On the basis of this approach, methods have been developed to significantly increase the optical modulation bandwidth. In this case, two lines are diffracted with high efficiency, and others – with Bragg synchronism detuning, i.e. with less efficiency [7, 8]. The total diffraction efficiency in this case can be quite high. In this paper, we describe the case of Bragg diffraction of radiation on a single acoustic wave propagating in a quartz crystal (α-SiO_2). This variant can be used to control multicolour radiation generated by an Ar laser in the blue-green region of the spectrum under condition of minimal distortion of the diffracted light. The paper compares the modulation characteristics of multicolour radiation using AO cells made of quartz and paratellurite (TeO_2). The advantage of AO cells made of quartz is that crystalline quartz is widely used in radioelectronics and technology of its production is well developed, which significantly reduces its cost. In addition, quartz, in contrast, for example, to paratellurite that includes toxic tellurium, is an environmentally friendly product.

V.M. Kotov, S.V. Averin, A.I. Voronko, P.I. Kuznetsov, S.A. Tikhomirov, G.N. Shkerdin, A.N. Bulyuk V.A. Kotel'nikov Institute of Radio Engineering and Electronics, Russian Academy of Sciences, Fryazino Branch, pl. akad. Vedenskogo 1, 141190 Fryazino, Moscow region, Russia; e-mail: vmk277@ire216.msk.su

Received 3 September 2014; revision received 29 June 2015
Kvantovaya Elektronika **45** (10) 942–946 (2015)
Translated by I.A. Ulitkin

2. Theory

It is known [1] that in the Bragg diffraction regime, the AO interaction of two plane waves, whose frequencies differ by Ω (where Ω is the sound frequency), is described by a system of differential equations

$$2\frac{dE_0}{dz} = -RE_1\exp(-i\Delta kz), \quad 2\frac{dE_1}{dz} = RE_0\exp(i\Delta kz), \qquad (1)$$

the solution of which under boundary conditions $E_0 = 1$ and $E_1 = 0$ at $z = 0$ has the form:

$$E_0 = \left[\cos\left(\sqrt{(\Delta k)^2 + R^2}\frac{L}{2}\right) + \frac{i\Delta k}{\sqrt{(\Delta k)^2 + R^2}} \times \sin\left(\sqrt{(\Delta k)^2 + R^2}\frac{L}{2}\right)\right]\exp\left(-\frac{i\Delta kL}{2}\right), \qquad (2)$$

$$E_1 = -\frac{R}{\sqrt{(\Delta k)^2 + R^2}}\sin\left(\sqrt{(\Delta k)^2 + R^2}\frac{L}{2}\right)\exp\left(\frac{i\Delta kL}{2}\right), \qquad (3)$$

where E_0 and E_1 are the field amplitudes of the zeroth and first diffraction orders, respectively; R is the parameter related to the acoustic power; Δk is the quantity of the Bragg synchronism detuning vector; z is the coordinate along which the AO interaction occurs; and L is the AO interaction length. Equations (1)–(3) are also valid for multicolour radiation diffraction under the assumption that the monochromatic components of radiation are diffracted on an acoustic wave independently. Then, Eqns (1)–(3) are written separately for each monochromatic component. It should be remembered that R, generally speaking, depends on the wavelength of light. If the wavelengths are close enough to each other, the wavelength dependence can be neglected. We describe here multicolour radiation generated by an Ar laser in the blue-green region of the spectrum. We also assume that R varies insignificantly with the wavelength.

An important parameter affecting the relationship between the E_0 and E_1 values is, as can be easily seen from (2) and (3), the synchronism detuning Δk, the value of which is determined on the basis of the analysis of wave vectors for a given vector of the acoustic wave [1].

Figure 1 shows the vector diagram of AO interaction. Optical radiation with the wave vector $\boldsymbol{K} = 2\pi\lambda^{-1}$ (λ is the wavelength of light) is incident on the optical face OX of the crystal at angle α. The face is oriented orthogonally to the optical axis OZ of the crystal. Inside the crystal, light is refracted and propagates with the wave vector $\boldsymbol{k}_\mathrm{i}$ at angle Θ_i to OZ. We assume that the diffraction occurs in a positive uniaxial crystal, and $\boldsymbol{k}_\mathrm{i}$ is the extraordinary ray. The ray $\boldsymbol{k}_\mathrm{i}$ interacts with an acoustic wave with the wave vector $\boldsymbol{q}$. Sound travels orthogonally to OZ. Figure 1 shows two variants of diffraction: when strict Bragg synchronism (wave vector $\boldsymbol{k}_\mathrm{d1}$ of the diffracted beam) and diffraction with synchronism detuning (vector $\boldsymbol{k}_\mathrm{d2}$) are fulfilled. We believe that the anisotropic diffraction occurs with a change in polarisation; rays $\boldsymbol{k}_\mathrm{d1}$ and $\boldsymbol{k}_\mathrm{d2}$ are ordinary. The synchronism detuning vector $\Delta\boldsymbol{k}$ closes the ends of the vectors $\boldsymbol{q}$ and $\boldsymbol{k}_\mathrm{d2}$, while it is directed orthogonally to the acoustic energy flow [9]. If the 'drift' of the acoustic beam is absent, the energy flow direction coincides with the direction of $\boldsymbol{q}$. In the geometry used by us, the 'drift' of the acoustic beam is absent. In this Figure we use the following notations: k_{x1} and k_{z1} are the projections of the vector $\boldsymbol{k}_\mathrm{i}$ on the directions OX and OZ, respectively; k_{x2} is the projection of the vector $\boldsymbol{k}_\mathrm{d1}$ on OX; and k_{x3} and k_{z3} are the projections of the vector $\boldsymbol{k}_\mathrm{d2}$ on OX and OZ. It is seen that $|\Delta k| = |k_{z3} - k_{z1}|$.

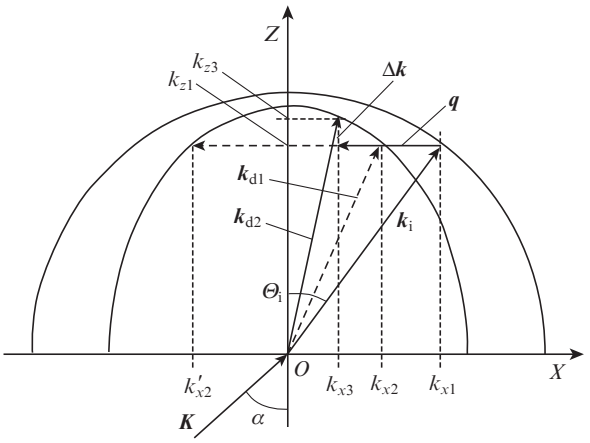

Figure 1. Vector diagram of AO interaction in a uniaxial gyrotropic crystal.

For specific values of Δk to be obtained, one must know the form of the wave surfaces of the crystal. The surfaces are determined from the dependence of the refractive index n on the angle Θ_i. The refractive indices of a uniaxial gyrotropic crystal, to which SiO_2 belongs, have the form

$$n_{1,2}^2 = (1+\tan^2\Theta_\mathrm{i})\left[\frac{1}{n_\mathrm{o}^2} + \frac{\tan^2\Theta_\mathrm{i}}{2}\left(\frac{1}{n_\mathrm{o}^2}+\frac{1}{n_\mathrm{e}^2}\right) \pm \frac{1}{2}\sqrt{\frac{\tan^4\Theta_\mathrm{i}}{2}\left(\frac{1}{n_\mathrm{o}^2}-\frac{1}{n_\mathrm{e}^2}\right)^2 + 4G_{33}^2}\right]^{-1}, \quad (4)$$

where n_o and n_e are the principal refractive indices of the crystal, and G_{33} is the component of the pseudo-tensor of gyration [6]. The dependences of n_o, n_e and G_{33} on the wavelength λ are obtained by interpolation of the tabulated values for SiO_2 [10, 11] and have the form

$$n_\mathrm{o} = \frac{0.003\times10^{-8}}{\lambda^2} + \frac{0.004\times10^{-4}}{\lambda} + 1.5287,$$
$$n_\mathrm{e} = \frac{0.0031\times10^{-8}}{\lambda^2} + \frac{0.0043\times10^{-4}}{\lambda} + 1.5371, \quad (5)$$
$$G_{33} = \frac{0.0052\times10^{-12}}{\lambda^2} + \frac{0.1053\times10^{-8}}{\lambda} - 0.0007\times10^{-4}.$$

From (4) we can find the surfaces of the wave vectors k of light in the crystal in the Cartesian coordinates:

$$k_z^4\left[\frac{1}{k_\mathrm{o}^4} - \left(\frac{\lambda}{2\pi}\right)^4 G_{33}^2\right] + k_x^2\left(\frac{1}{k_\mathrm{o}^2}+\frac{1}{k_\mathrm{e}^2}\right)\left(\frac{k_z^2}{k_\mathrm{o}^2}-1\right) + \frac{k_x^4}{k_\mathrm{o}^2k_\mathrm{e}^2} - \frac{2k_z^2}{k_\mathrm{o}^2} + 1 = 0, \quad (6)$$

where $k_\mathrm{o} = (2\pi/\lambda)n_\mathrm{o}$; $k_\mathrm{e} = (2\pi/\lambda)n_\mathrm{e}$; and k_x and k_z are the projections of the wave vector of light propagating in the crystal on the axes OX and OZ, respectively, so that $|k|^2 = k_x^2 + k_z^2$. According to Snell's law, the projection of k_i on the direction of OX is $k_{x1} = K\sin\alpha$. Expressing k_z by k_x (6), we obtain a biquadratic equation of the form

$$A_1K_z^4 + B_1k_z^2 + C_1 = 0, \quad (7)$$

where

$$A_1 = \frac{1}{k_\mathrm{o}^4} - \left(\frac{\lambda}{2\pi}\right)^4 G_{33}^2; \quad B_1 = \frac{1}{k_\mathrm{o}^2}\left[k_x^2\left(\frac{1}{k_\mathrm{o}^2}+\frac{1}{k_\mathrm{e}^2}\right) - 2\right];$$
$$C_1 = \frac{k_x^4}{k_\mathrm{o}^2k_\mathrm{e}^2} - k_x^2\left(\frac{1}{k_\mathrm{o}^2}+\frac{1}{k_\mathrm{e}^2}\right) + 1. \quad (8)$$

Substituting $k_x = k_{x1} = K\sin\alpha$ into (7), (8), we obtain the projection k_{z1} of radiation k_i on the direction of OZ:

$$k_{z1}^2 = -\frac{B_1}{2A_1} \pm \sqrt{\left(\frac{B_1}{2A_1}\right)^2 - \frac{C_1}{A_1}}. \quad (9)$$

Of the four possible roots of k_{z1} we take the maximum one corresponding to the extraordinary ray. To obtain frequency-angular characteristics of AO interaction it is necessary to find the frequency of sound at a given angle of incidence α and implementation of strict Bragg synchronism. To do this, in (6) we express k_x through k_z. We obtain a biquadratic equation of the form

$$A_2k_x^4 + B_2k_x^2 + C_2 = 0, \quad (10)$$

where

$$A_2 = \frac{1}{k_\mathrm{o}^2k_\mathrm{e}^2}; \quad B_2 = \left(\frac{1}{k_\mathrm{o}^2}+\frac{1}{k_\mathrm{e}^2}\right)\left(\frac{k_z^2}{k_\mathrm{o}^2}-1\right);$$
$$C_2 = k_z^4\left[\frac{1}{k_\mathrm{o}^4} - \left(\frac{\lambda}{2\pi}\right)^4 G_{33}^2\right] - \frac{2k_z^2}{k_\mathrm{o}^2} + 1; \quad (11)$$

$$k_{x2}^2 = -\frac{B_2}{2A_2} \pm \sqrt{\left(\frac{B_2}{2A_2}\right)^2 - \frac{C_2}{A_2}}. \quad (12)$$

Among the four possible values of k_{x2} we choose two, which describe the ordinary ray. The corresponding roots – k_{x2} and k'_{x2} – are equal and opposite in sign. Then, high-fre-

quency and low-frequency branches of the frequency-angular dependences are expressed as

$$f_{\max} = \frac{V}{2\pi}(K\sin\alpha + |k_{x2}|), \quad f_{\min} = \frac{V}{2\pi}(K\sin\alpha - |k_{x2}|)$$

(V is the speed of sound).

We have chosen the low frequency branch, because in this case the frequency-angular characteristics of the Ar-laser emission lines are most close to each other. In addition, the angle between the diffracting rays is small, so that all the rays are simply collected by a prism to form a beam. In other words, the proposed configuration introduces minimal distortions in the composition of the polychromatic beam. The upper limit of the low-frequency branch is determined by the frequency of double Bragg diffraction, and the lower limit – by the condition of the existence of the Bragg regime. We have chosen a range that lies fairly close to the upper limit. Figure 2a shows the dependence of the sound frequency f on the angle α for five Ar-laser wavelengths propagating in a quartz crystal. For comparison, Fig. 2b shows the same dependences for a TeO_2 crystal. The values of n_o, n_e and G_{33} at different wavelengths λ for TeO_2 are taken from [12].

Curves (*1*)–(*5*) in Fig. 2 correspond to the Ar-laser wavelengths of 0.477, 0.488, 0.496, 0.501 and 0.514 μm. For SiO_2 we used the frequency of 60 MHz (Fig. 2a). A similar frequency for TeO_2, providing similar frequency-angular dependences for SiO_2, is, in our opinion, the frequency of 35 MHz (Fig. 2b). The comparison of the figures shows that the range of angles covered by the given wavelengths for SiO_2 at the selected frequency is about four times less than the range of angles for TeO_2. An even greater difference arises in finding the detuning $|\Delta k|$ for both crystals. To find $|\Delta k|$ from Fig. 1, we note that the projection $k_{x3} = K\sin\alpha - q$. Hence, substituting k_{x3} into (7)–(9), we obtain k_{z3} and $|\Delta k| = |k_{z3} - k_{z1}|$.

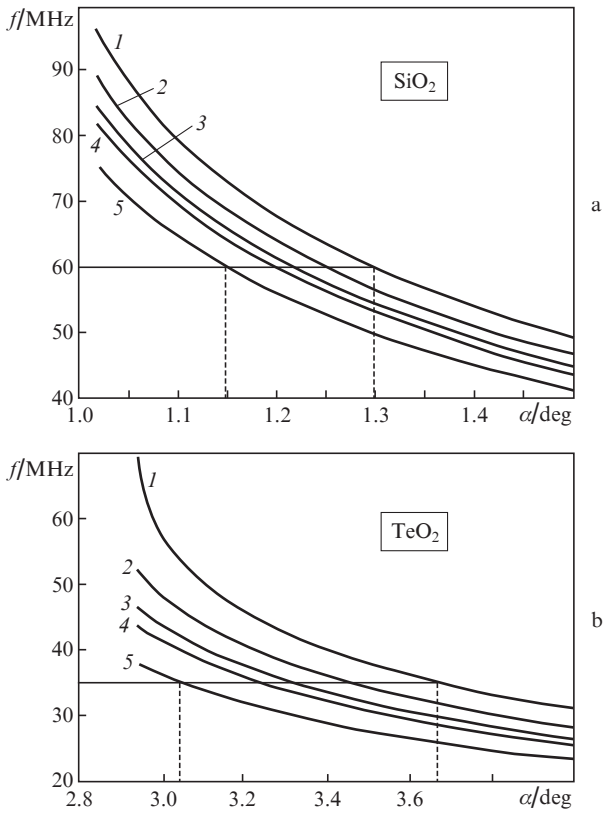

Figure 2. Dependences of the sound frequency f on the angle α of light incidence on the (a) SiO_2 and (b) TeO_2 crystals for Ar-laser emission lines at wavelengths of (*1*) 0.477, (*2*) 0.488, (*3*) 0.496, (*4*) 0.501 and (*5*) 0.514 μm.

Figure 3 shows the dependences of $|\Delta k|$ on λ: the dependences for SiO_2 and TeO_2 are plotted at the sound frequencies f = 60 and 35 MHz, respectively. Selecting the angle α of incidence of light provides a situation when $|\Delta k| = 0$ for λ = 0.5 μm (average Ar-laser wavelength) for both crystals. It can be seen that for TeO_2 $|\Delta k|$ changes almost an order of magnitude greater than for SiO_2. Therefore, the diffraction efficiency of Ar-laser lines in the case of using TeO_2, as follows from (2), will be highly inhomogeneous. Such a large difference in the frequency-angular characteristics and behaviour of $|\Delta k|$, in our opinion, is associated with a stronger optical anisotropy of TeO_2 [the value of $(n_e - n_o)/n_o$] than the anisotropy of SiO_2.

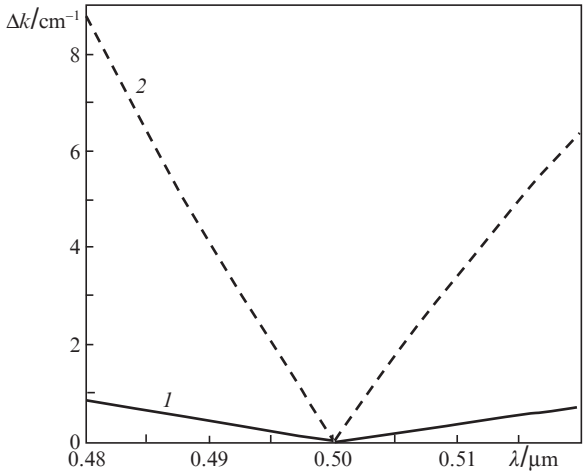

Figure 3. Dependences of the phase mismatch vector Δk on the light wavelength λ for (*1*) SiO_2 and (*2*) TeO_2.

3. Experiment and discussion of its results

The experiment was carried out using an AO cell made of SiO_2. The crystal faces were oriented perpendicularly to the directions (100), (010) and (001). A $LiNbO_3$ piezoelectric transducer generating transverse acoustic waves with a centre frequency of 60 MHz and a bandwidth of 20% was glued to the [010] face. The AO interaction length was L = 0.6 cm. The transverse wave with the direction of displacement along [100] propagated in the crystal. The velocity of sound measured experimentally was equal to 3.834×10^5 cm s^{-1}, and the voltage at the transducer was 15 V. Multicolour radiation from the Ar laser was directed to the cell. The diffraction efficiency was ~5% in all lines, all lines diffracting almost simultaneously: they simultaneously appeared and disappeared when changing the angle of light incidence on the cell.

For comparison, experiments were performed with a TeO_2 cell excited at a sound frequency of 35 MHz. The applied voltage was 4 V, and the speed of sound was equal to 0.617×10^5 cm s^{-1}. In experiments with TeO_2, we managed to achieve efficient diffraction of a small portion of the total radiation, in fact – only one emission line of the Ar laser. We

studied the brightest line (0.514 μm), for which the diffraction efficiency reached 50%. For radiations at other wavelengths to be diffracted, it was necessary to change the angle of light incident on the crystal. Thus, it was experimentally confirmed that at the same AO interaction length and diffraction geometry, the use of the SiO_2 crystal allows five lines of the Ar-laser radiation to be deflected, as compared to only one line in the case of TeO_2. In the latter case, it would be possible to cover all the lines by significantly reducing the AO interaction length, but it leads to a distortion of the shape of diffracted beams [1, 13], as well as to the emergence of other 'undesirable' diffraction orders.

In the next series of experiments, SiO_2 and TeO_2 cells were compared as AO modulators. We measured and compared the shapes of the electric and optical signals when an electrical pulse was applied to the input of the AO cell. Figure 4a shows photographs of an electric signal applied to the SiO_2 cell (top) and of an optical signal measured at the output of a fast photodetector (bottom). The duration of the electrical signal was ~6 μs, the frequency was 60 MHz, the applied pulse voltage was 40 V and the duty ratio was 100. It can be seen that the slope of the leading and trailing edges of the optical signal sufficiently well repeats the slope of the electric pulse.

Similar measurements were performed using the TeO_2 cell (Fig. 4b) for the same duration of the electrical signal, but for a frequency of 35 MHz at an applied voltage of 4 V. Because of the high diffraction selectivity of TeO_2 to the wavelength of light, we used only one emission line of the Ar laser: λ = 0.514 μm. The voltage applied to the TeO_2 cell was 10 times smaller than the voltage applied to the SiO_2 cell, which is due to the fact that the AO quality factor M_2 of the SiO_2 crystal is about 1000 times smaller than M_2 of the TeO_2 crystal. The pulses were generated by the same generator, but an increase in the voltage pulse led to its distortion. In our case it was not significant, since it was important to compare the shape of an electric signal applied to the cell with the shape of an optical output signal. The comparison of waveforms for the TeO_2 cell shows that the shape of the optical signal does not follow the shape of the electric one: the fronts of the optical signal are not as steep as those of the electric one. The distortion of the fronts is caused by a low-speed passage of the sound pulse through the aperture of the light beam. In the case of SiO_2 this is not observed, because the speed of sound in SiO_2 is about six times more than in TeO_2.

4. Conclusions

Based on the above-said, we can draw the following conclusions.

1. To control multicolour optical radiation by AO diffraction in a uniaxial gyrotropic crystal, it is proposed to use the low-frequency branch of the frequency-angular dependence, which, in combination with a prism collecting all the diffracted beams into a single beam, introduces a minimal distortion in the composite polychromatic beam.

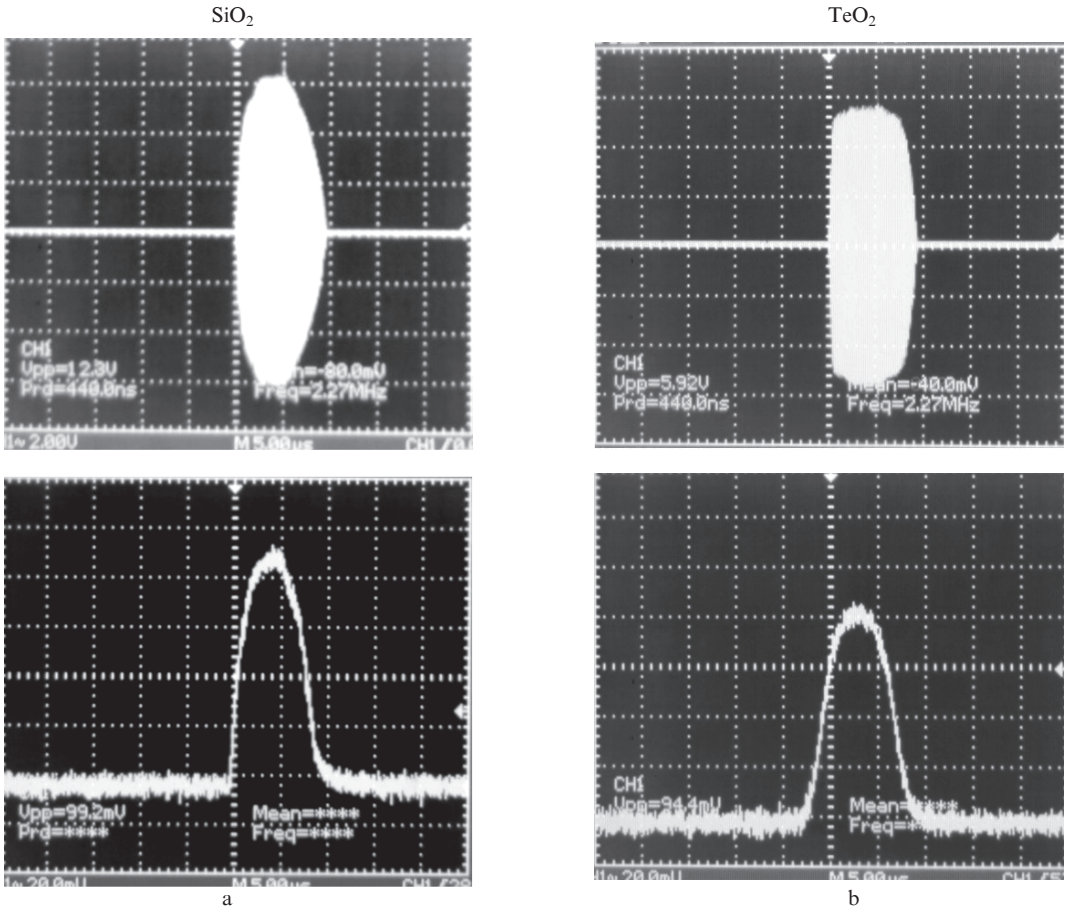

Figure 4. Electrical signal applied to the AO cell made of SiO_2 or TeO_2 (a, b; top) and optical signal measured at the output of the cells (a, b; bottom).

2. It is shown that in terms of the phase mismatch, the use of a quartz crystal for multicolour radiation modulation is preferable to the use of paratellurite, which is primarily due to a higher anisotropy of TeO_2, as compared to that of SiO_2.

3. It is shown experimentally that at the working frequency of sound, the multicolour Ar-laser radiation in the SiO_2 crystal is diffracted almost simultaneously for all the rays of the spectral range, whereas in TeO_2, having the same geometry and the same length of AO interaction, AO diffraction is highly selective to optical wavelengths.

4. AO modulators made of SiO_2 and TeO_2 are compared. It is shown that the optical pulse fronts produced by a SiO_2 modulator transfer the electric pulse fronts much better than a TeO_2 modulator, which is due to a significant difference in the speeds of sound in these crystals.

In conclusion, we would like to add that the final choice of the AO cell material is always left to discretion of the experimenter. It is determined by the conditions and specifics of the experiment, the technical requirements, preferences of the experimenter, etc. If, according to the requirements, high resistance of the crystal to the effects of laser radiation is needed, quartz is beyond comparison. In this paper, we have demonstrated another advantage of quartz – minimum desynchronisation of the beams of polychromatic radiation from the acoustic wave. Some experimenters, nevertheless, prefer using paratellurite in these cases by solving, in particular, the problem of desynchronisation of rays by increasing the sound wave divergence and the acoustic power. It is clear that it is necessary to solve the problem of increasing TeO_2 resistance to high-power laser radiation. Both approaches are legitimate, and each has advantages and disadvantages. But as is known, different approaches to solving the same problem only complement each other and help to deal more effectively with the task.

Acknowledgements. This work was supported by the Russian Foundation for Basic Research (Grant No. 13-07-00138) and the RF President's Grants Council (State Support to Leading Scientific Schools Programme, Grant No. NSh-3317.2010.9).

References

1. Balakshii V.I., Parygin V.N., Chirkov L.E. *Fizicheskie osnovy akustooptiki* (Physical Foundations of Acoustic Optics) (Moscow: Radio i Svyaz', 1985).
2. Xu J., Stroud R. *Acousto-optic Devices: Principles, Design, and Applications* (New York: John Wiley & Son Inc., 1992).
3. Yariv A., Yeh P. *Optical Waves in Crystals* (New York: Wiley, 1984; Moscow: Mir, 1987).
4. Kotov V.M. *Zh. Tekh. Fiz*., **62** (8), 95 (1992).
5. Kotov V.M. *Opt. Spektrosk*., **74** (2), 386 (1993).
6. Kotov V.M. *Opt. Spektrosk*., **77** (3), 493 (1994).
7. Kotov V.M. *Zh. Tekh. Fiz*., **66** (1), 151 (1996).
8. Kotov V.M. *Usp. Prikl. Fiz*., **2** (2), 177 (2014).
9. Balakshii V.I., Mantsevich S.N. *Opt. Spektrosk*., **103** (5), 831 (2007).
10. Shaskolskaya M.P. (Ed.) *Akusticheskie kristally* (Acoustic Crystals) (Moscow: Nauka, 1982).
11. Kizel' V.A., Burkov V.I. *Girotropiya kristallov* (Gyrotropy of Crystals) (Moscow: Nauka, 1980).
12. Kotov V.M. *Prikl. Fiz*., (2), 69 (2014).
13. Magdich L.N., Molchanov V.Ya. *Akustoopticheskie ustroistva i ikh primeneniya* (Acousto-Optical Devices and Their Application) (Moscow: Radio i Svyaz', 1978).